# Phase-Based UHF RFID Tracking With Nonlinear Kalman Filtering and Smoothing

Simo Särkkä, *Member, IEEE*, Ville V. Viikari, *Senior Member, IEEE*, Miika Huusko, and Kaarle Jaakkola

***Abstract*—In this paper, we present an UHF RFID location tracking system, which is based on measuring the phases of backscattered signals from RFID tag using multiple spatially distributed antennas at a single carrier frequency. The wavelength ambiguity of the phase measurements is resolved by using the extended Kalman filter (EKF) and the Rauch-Tung-Striebel (RTS) smoother, where the state includes the position, velocity and the phase offsets of antennas. The performance of the method is experimentally verified at 890 MHz using a commercially available RFID reader.**

***Index Terms*—Extended Kalman filter, RFID, RTS smoother, tracking, transponders, wireless sensors.**

## I. Introduction

FUTURE ubiquitous sensing, manufacturing, and computing systems will necessitate automatic location sensing. Examples include indoor localization of people (e.g., customers in a mall, medical personnel and patients in a hospital, and first responders and victims in a rescue operation) and asset tracking (e.g., products in a warehouse and equipment and machinery in a laboratory or a workshop).

Location sensing utilizes typically microwaves, visible light or infrared [1]–[3], or sound [4]. The advantages of microwaves over other sensing principles include long range (e.g., the GPS), operation in dark and adverse conditions, immunity to wind, and no need for a line-of-sight between the object and the sensing system. Reviews of location sensing systems can be found in [5]–[7].

RFID is almost exclusively used for identification, but could offer several advantages as a short range location sensing system. RFID tags are very inexpensive and offer sophisticated features including nonvolatile memory and anti-collision protocols. In addition, reader infrastructure already exists in many locations.

RFID has been traditionally used for proximity location sensing. Enhanced accuracy is obtained estimating the distance from the signal attenuation, that is, using the received signal strength indicator (RSSI) [8]–[11]. In the RSSI-based methods, only free space attenuation is assumed and other unknown attenuation mechanisms affecting the signal level, such as polarization mismatch, multipath propagation and antenna gain variation due to tag alignment cause large distance errors.

The phase of the backscattered signal can also be exploited for enhanced positioning accuracy, see for example a review of RFID phase-based location methods [14]. The phase-based positioning methods can be divided into time-, frequency-, and spatial domain (TD, FD, SD) methods. The time-domain methods can solve the axial velocity of the tag based on the Doppler-frequency (phase-difference of the backscattered signal at different time instants). However, the method does not give information on the absolute position of the tag.

In frequency-domain methods, the distance of an RFID tag is measured by sweeping the carrier frequency [12]. An accurate distance measurement, however, necessitates a bandwidth that does not comply with the frequency regulations set for RFID in Europe (865 MHz – 868 MHz) [13].

Spatial domain methods exploit spatially diverse antennas and beam-forming for solving the tag's location. Narrow-band beam-forming techniques, however, suffer from the position ambiguity due to unknown number of full wavelengths. In narrow-band systems, such as in UHF RFID, spatial methods can only be used to measure the direction to the tag, but not the distance. In this paper, we present an RFID-based tracking system, which operates using phase measurements from multiple spatially distributed reader antennas at a single frequency. The phase ambiguity biases (that is the unknown number of full wavelengths between the object and the reader) related to continuous wave (CW) measurements are solved by applying a state-space model using the position, velocity and the phase offsets as components. The estimation of the whole state trajectory is then performed with extended Kalman filter (EKF) and Rauch-Tung-Striebel (RTS) smoother (see, e.g., [15] and [16]). The method combines the spatial- and time-domain positioning techniques utilizing a dynamical model for the target and can thus provide both the velocity and absolute position of the tag, which cannot be solved using any single positioning method. It is also straightforward to exploit broad-band measurements (frequency domain) with the method if needed.

The tracking system is being developed for purposes of biological studies aiming to follow the activity and movements of a butterfly called Granville Fritillary (*Melitaea cinxia*) in an indoor cage. The first generation of the UHF RFID-based butterfly tracking system is presented in [10] and a photograph of a butterfly equipped with a UHF RFID transponder is shown in Fig. 1. In addition to insect tracking for biological studies, the system could be used in various other applications including indoor positioning and asset tracking.

Several remote sensing and telemetric insect tracking techniques have been developed for the demands of biological and agricultural studies [17]. The proposed techniques in-

Manuscript received June 15, 2011; accepted July 15, 2011. Date of publication August 08, 2011; date of current version April 06, 2012. This work was supported in part by the Academy of Finland under the decision 132982 and in part by the EU Commission under ADOSE project Contract FP7-ICT-2007-1-216049. The associate editor coordinating the review of this paper and approving it for publication was Prof. K. Kim.

S. Särkkä is with the Aalto University, 02150 Espoo, Finland (e-mail:simo.sarkka@tkk.fi).

V. V. Viikari, M. Huusko and K. Jaakkola are with VTT Technical Research Centre, 02044 Espoo, Finland (e-mail: ville.viikari@vtt.fi, miika.huusko@vtt.fi, kaarle.jaakkola@vtt.fi).

Color versions of one or more of the figures in this paper are available online at http://ieeexplore.ieee.org.

Digital Object Identifier 10.1109/JSEN.2011.2164062

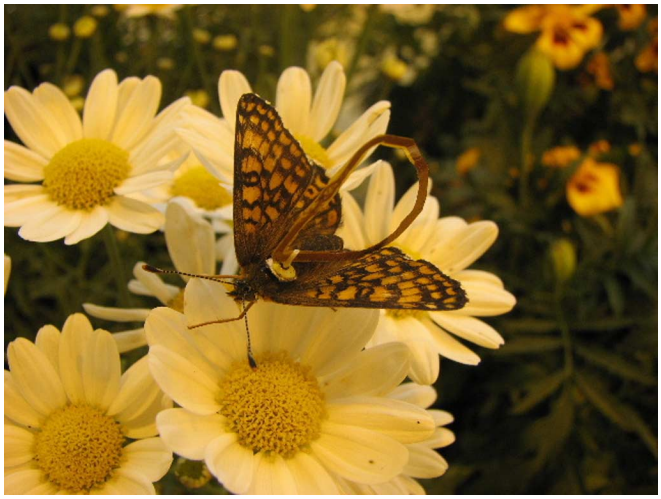

Fig. 1. Butterfly equipped with an UHF RFID transponder.

clude radar, video graphic and other optical techniques, X-ray imaging, and passive and active acoustical techniques. One of the most common techniques is the secondary or harmonic radar [18], in which the tracked objects are equipped with a passive transponder that scatters harmonic products of radar signal. Harmonic radar for insect tracking is discussed in [19]–[21] and the concept is also utilized in other wireless sensors [22]–[25].

An advantage of the RFID tracking principle over almost all other insect tracking techniques is that RFID can be used to track and identify multiple targets simultaneously. In addition, the RFID-based location sensing system is realized in a straightforward way using commercially available RFID reader.

## II. Location Sensing System

The location sensing system consists of spatially distributed RFID reader antennas in known locations. Each antenna measures the complex response of the tag (phase and amplitude of the modulated backscatter). When the tag moves relative to the antennas, its position is solved using a state space model for the target.

### A. Spatial Response of the Tag

Consider isotropic and identical RFID reader antennas at fixed positions $\mathbf{a_i}$ and an RFID tag, whose position at a time $t$ is $\mathbf{p}(t)$. The reader illuminates the tag by a continuous wave (CW) from one antenna at a time and the tag produces modulated backscattering by alternating its reflection coefficient. Assuming an isotropic tag antenna and the free-space attenuation to the signal and neglecting possible multipath propagation effects and polarization mismatch, the measured modulated response of the tag from $i$th antenna is given as

$$\Delta Y_i(t_n) = \frac{A_0}{\left|\mathbf{p}(\mathrm{t}_n) - \mathbf{a_i}\right|^2} e^{-j(2\omega/c)\left|\mathbf{p}(t_n) - \mathbf{a_i}\right|} + \varepsilon_i(t_n) \quad (1)$$

where $A_0$ is a complex gain constant, $\omega$ is the angular frequency, $c$ is the speed of light, and $\varepsilon_i$ is a noise term.

### B. Estimating Pseudo-Distances From Phase

If we assume that the measurement noise is small, we can compute an estimate of the distance from the instantaneous phase

$$\angle \Delta Y_i(t_n) = \frac{2\omega}{c}\left|\mathbf{p}(\mathrm{t}_n) - \mathbf{a_i}\right| + 2\pi N_i \quad (2)$$

where $N_i$ is the unknown number of multiples of a half of the wave length. Solving for the distance $r_i$ between the $i$th antenna and the tag at $t_n$ gives

$$r_i(t_n) = \left|\mathbf{p}(\mathrm{t}_n) - \mathbf{a_i}\right| = -\frac{c}{2\omega}\angle \Delta Y_i(t_n) + \frac{c\pi N_i}{\omega} \quad (3)$$

where the integer $N_i$ is unknown. Assuming that the speed of the tag does not exceed $\lambda/(2(t_{n+1} - t_n))$ (i.e., the tag is not displaced more than half wavelength between adjacent measurements) we can compute an estimate of the distance, or the pseudo-distance using the following recursion:

$$\widehat{r}_i(t_n) = \widehat{r}_i(t_{n-1}) - \frac{c}{2\omega}\angle\left\{\frac{\Delta Y_i(t_n)}{\Delta Y_i(t_{n-1})}\right\}. \quad (4)$$

The recursion can be started from some guess of the initial position $\widehat{\mathbf{p}}(t_0)$ as follows:

$$\widehat{r}_i(t_0) = \left|\widehat{\mathbf{p}}(\mathrm{t}_0) - \mathbf{a_i}\right|. \quad (5)$$

The computed pseudo-distance will then have an unknown offset $b_i$ with respect to the actual distance

$$\widehat{r}_i(t_n) = \left|\mathbf{p}(\mathrm{t}_n) - \mathbf{a_i}\right| + b_i. \quad (6)$$

Actually, the constant is of the form $b_i = c\pi k_i/\omega$ where $k_i$ is an antenna-specific integer, but we shall simply consider it as a constant real number.

### C. State Space Model for Dynamic Tracking

Consider the following Wiener velocity model or continuous white noise acceleration (CWNA) model [15]

$$\frac{d^2\mathbf{p}(t)}{dt^2} = \mathbf{w_v}(t) \quad (7)$$

where $\mathbf{w_v}(t)$ is a continuous time white noise process with spectral density $\mathbf{Q_v} = q_v\mathbf{I}$, where the constant $q_v$ models the assumed amount of perturbations on the path. By introducing the temporally varying velocity $\mathbf{v}(t) = d\mathbf{p}(\mathrm{t})/dt$, the model can be written in the following state space form:

$$\frac{d}{dt}\begin{pmatrix}\mathbf{p}(t)\\ \mathbf{v}(t)\end{pmatrix} = \begin{pmatrix}\mathbf{0} & \mathbf{I}\\ \mathbf{0} & \mathbf{0}\end{pmatrix}\begin{pmatrix}\mathbf{p}(t)\\ \mathbf{v}(t)\end{pmatrix} + \begin{pmatrix}\mathbf{0}\\ \mathbf{I}\end{pmatrix}\mathbf{w_v}(t). \quad (8)$$

Although the biases $b_i$ remain constants from physical grounds, they are modeled as variables with a random walk (Brownian motion). This approach is chose to assure the convergence of the estimation across phase wraps.The biases at different time instants are related by

$$\frac{db_i(t)}{dt} = w_{bi}(t) \quad (9)$$

where $w_{bi}(t)$ is a continuous time white noise process with (small) spectral density $q_b$. Let us now define state $\mathbf{x}(t)$ as follows (here $d = 2$ for 2d-tracking and $d = 3$ for 3d):

$$\mathbf{x}(t) = (p_1, \ldots, p_d, b_1, \ldots, b_s, v_1, \ldots, v_d). \tag{10}$$

In terms of the state, the dynamic model and measurement model can be combined into the following continuous-discrete state space model:

$$\begin{aligned} \frac{d\mathbf{x}(t)}{dt} &= \mathbf{F}\mathbf{x}(t) + \mathbf{L}\mathbf{w}(t) \\ \widehat{r}_i(t_n) &= h_i(\mathbf{x}(t_n)) + \epsilon_i \end{aligned} \tag{11}$$

where $i = 1, \ldots, s$, (and $s$ is the number of the reader antenna) and $\epsilon_i$ is Gaussian noise related to the measurements

$$\begin{aligned} \mathbf{F} &= \begin{pmatrix} \mathbf{0} & \cdots & \mathbf{I} \\ \vdots & \ddots & \\ \mathbf{0} & & \mathbf{0} \end{pmatrix} \quad \mathbf{L} = \begin{pmatrix} \mathbf{0} \\ \mathbf{I} \end{pmatrix} \\ h_i(\mathbf{x}) &= \left|\mathrm{p} - \mathrm{a}_{\boldsymbol{i}}\right| + b_i \end{aligned} \tag{12}$$

and $\mathbf{w}(t)$ is a white noise process with spectral density $\mathbf{Q} = \mathrm{diag}(q_b, \ldots, q_b, q_v, \ldots, q_v)$.

### *D. Estimating the Initial Position of the Tag*

The initial position of the tag is estimated using the received signal attenuation indicator (RSSI), although other estimation methods are possible too. According to our experiments, even a very coarse initial position estimate is sufficient. The algorithm rapidly converges to the correct place if the center of the tracking area is used as the initial position and the covariance matrix is set to represent a Gaussian distribution covering the whole observation area.

In our experiments, the initial position is estimated from logarithmic received signal strength assuming free-space propagation conditions. The position is calculated as

$$\min_{\mathbf{p}} \sum_i \left[ \ln \frac{A_0}{\left|\mathbf{p} - \mathbf{a}_{\boldsymbol{i}}\right|^2} \cdot \frac{1}{|Y_i|} \right]^2 \tag{13}$$

where $A_0$ is a gain constant, $\mathbf{p}$ is the initial position, $\mathbf{a}_i$ is the position of the $i$th reader antenna, and $Y_i$ is the measured response of the tag. Logarithmic least squares estimation is chosen because it provides better accuracy than a linear least squares fit under multipath propagation conditions.

### *E. Estimating the Trajectory of the Tag*

The state-space model is converted into more compatible form by forming a weak solution to the stochastic differential equation at the measurement steps as

$$\begin{aligned} \mathbf{A}_n &= e^{\mathbf{F}\Delta t_n} \\ \mathbf{W}_n &= \int_{\mathbf{0}}^{\Delta t_n} e^{\mathbf{F}(\Delta t_n - \tau)} \mathbf{L}\mathbf{Q}\mathbf{L}^{\boldsymbol{T}} e^{\mathbf{F}^{\boldsymbol{T}}(\Delta t_n - \tau)} d\tau \end{aligned} \tag{14}$$

where $\Delta t_n = t_{n+1} - t_n$. Let us also combine the measurements from individual antennas into a single vector $\mathbf{z}_n = (\widehat{r}_1(t_n), \ldots, \widehat{r}_s(t_n))$, and further define $\mathbf{h}(\mathbf{x}) = (h_1(\mathbf{x}), \ldots, h_s(\mathbf{x}))$ and $\boldsymbol{\epsilon} = (\epsilon_1, \ldots, \epsilon_s)$. Then, the model can be written as a standard discrete-time nonlinear Gaussian state space model

$$\begin{aligned} \mathbf{x}(t_{n+1}) &= \mathbf{A}_n \mathbf{x}(t) + \mathbf{w}_n, \quad \mathbf{w}_n \sim \mathrm{N}(\mathbf{0}, \mathbf{W}_n) \\ \mathbf{z}_n &= \mathbf{h}(\mathbf{x}(t_n)) + \boldsymbol{\epsilon}. \end{aligned} \tag{15}$$

The standard state estimation algorithms such as EKF and RTS smoother can be used for estimating the state from the measurements. Note that perfectly concurrent measurements form different antennas are assumed for simplicity. The extension to the nonsynchronized case is straightforward.

The EKF algorithm processes the measurements one at a time and at each measurement, performs the following prediction and update steps for each $n = 1, 2, 3, \ldots$.

Prediction:

$$\begin{aligned} \widehat{\mathbf{x}}^-(t_n) &= \mathbf{A}_{n-1} \widehat{\mathbf{x}}(t_{n-1}) \\ \mathbf{P}^-(t_n) &= \mathbf{A}_{n-1} \mathbf{P}(t_{n-1}) \mathbf{A}_{n-1}^T + \mathbf{W}_{n-1}. \end{aligned} \tag{16}$$

Update:

$$\begin{aligned} \mathbf{S}_n &= \mathbf{H}_{\boldsymbol{x}}(\widehat{\mathbf{x}}^-(t_n)) \mathbf{P}^-(t_n) \mathbf{H}_{\boldsymbol{x}}^T(\widehat{\mathbf{x}}^-(t_n)) + \sigma^2 \mathbf{I} \\ \mathbf{K}_n &= \mathbf{P}^-(t_n) \mathbf{H}_{\boldsymbol{x}}^T(\widehat{\mathbf{x}}^-(t_n)) \mathbf{S}_n^{-1} \\ \widehat{\mathbf{x}}(t_n) &= \widehat{\mathbf{x}}^-(t_n) + \mathbf{K}_n \left[\mathbf{z}_n - \mathbf{h}(\widehat{\mathbf{x}}^-(t_n))\right] \\ \mathbf{P}(t_n) &= \mathbf{P}^-(t_n) - \mathbf{K}_n \mathbf{S}_n \mathbf{K}_n^T \end{aligned} \tag{17}$$

where $\mathbf{H}_{\boldsymbol{x}}(\mathbf{x})$ denotes the Jacobian matrix of $\mathbf{h}(\mathbf{x})$. The initial estimate $\widehat{\mathbf{x}}(t_0)$ and its covariance $\mathbf{P}(t_0)$ encode the prior information about the initial position.

The EKF only computes *causal* estimates, which means that the estimates are conditioned only on the previous and current measurements, not on the measurements obtained after a given step $n$. After obtaining a set of measurements $\mathbf{z}_1, \ldots, \mathbf{z}_N$ it is also possible to compute MMSE estimate of the whole trajectory, which is conditioned on all the measurements

$$\widehat{\mathbf{x}}^s(t_n) = \mathrm{E}[\mathbf{x}(t_n) \mid \mathbf{z}_1, \ldots, \mathbf{z}_N] \tag{18}$$

where $N$ is the number of measurements. The estimate can be computed with the RTSl smoother (see, [16]). Because the estimates are conditioned on the whole set of measurements, it provides higher precision than the filtering estimates. After the filtering estimates have been computed, the smoothed state estimate and its covariance can be computed with the following backward recursion for $n = N - 1, \ldots, 0$:

$$\begin{aligned} \widehat{\mathbf{x}}^-(t_{n+1}) &= \mathbf{A}_n \widehat{\mathbf{x}}(t_n) \\ \mathbf{P}^-(t_{n+1}) &= \mathbf{A}_n \mathbf{P}(t_n) \mathbf{A}_n^T + \mathbf{W}_n \\ \mathbf{G}_n &= \mathbf{P}(t_n) \mathbf{A}_n^T [\mathbf{P}^-(t_{n+1})]^{-1} \\ \widehat{\mathbf{x}}^s(t_n) &= \widehat{\mathbf{x}}(t_n) + \mathbf{G}_n \left[\widehat{\mathbf{x}}^s(t_{n+1}) - \widehat{\mathbf{x}}^-(t_{n+1})\right] \\ \mathbf{P}^s(t_n) &= \mathbf{P}(t_n) + \mathbf{G}_n [\mathbf{P}^s(t_{n+1}) - \mathbf{P}^-(t_{n+1})] \mathbf{G}_n^T. \end{aligned} \tag{19}$$

The recursion is started from the filter results at the last time step: $\widehat{\mathbf{x}}^s(t_N) = \widehat{\mathbf{x}}(t_N)$, $\mathbf{P}^s(t_N) = \mathbf{P}(t_N)$.

When the data set is limited and the assumed initial position differs significantly from the true initial position, it is possible that the bias estimation does not converge close enough to the true bias during one run of the filter and the smoother. Then, it is possible to iteratively run the filter and smoother back and forth

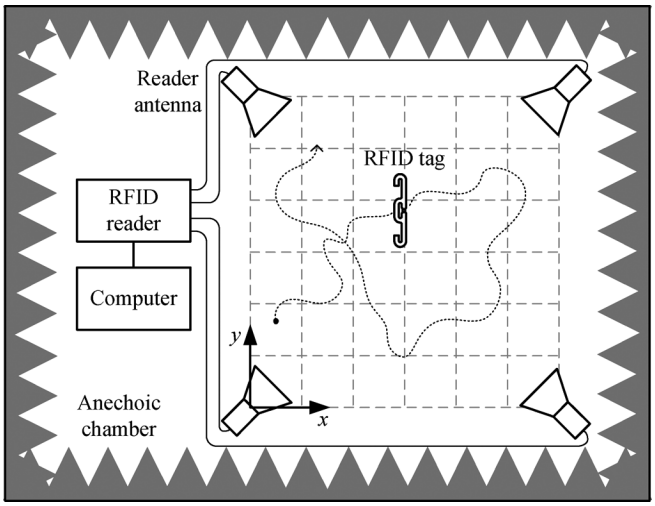


Fig. 2. Measurement setup for tracking an object equipped with an RFID tag.

until the change in the bias between adjacent iterations is below a predetermined threshold value.

The used linear model for the target dynamics and relatively simple measurement model are suitable for the basic EKF. If nonlinear model for the dynamics or other type of measurement than phases should be incorporated, the tracking could be realized using unscented Kalman filters [26], [27], more general Gaussian integration based filters [28], [29] or corresponding smoothers [30], [31] in the estimation instead.

## III. Experiments

### A. Measurement Setup

The UHF RFID based location sensing system is tested in an anechoic chamber before an installation in the indoor butterfly cage. Four reader antennas (SPA 8090/75/8/0/V, Huber Suhner, Switzerland) are located at the corners of a square with 3 m face length. The antennas are 1.5 m above floor and they are directed towards the center of the square.

The tracked RFID tag (Dogbone, UPM RFID, Pirkkala, Finland) is mounted on a movable stand at 1.5 m height. The tag is moved by manually sliding the stand along a predefined trajectory marked on the floor.

The response of the tag from each antenna is measured at 890 MHz with an RFID reader (INfinity™ 510 UHF Reader, Sirit Inc., Toronto, Canada). An average read-out speed of the reader is 400 times per second (100 read-outs per second from each reader antenna). Fig. 2 shows a schematic layout and Fig. 3 a photograph of the measurement setup.

### B. Measured Response of the Tag

Fig. 4 shows the pseudo-distances of the tag from different reader antennas during one experiment. The pseudo-distances have been calculated from the raw phase measurements using the procedure described in Section II-B and thus they contain an unknown constant offset. The pseudo-distances from different antennas change smoothly in time and no discontinuities due to possible phase-wraps are seen. Furthermore, no significant random noise can be observed on the curves.

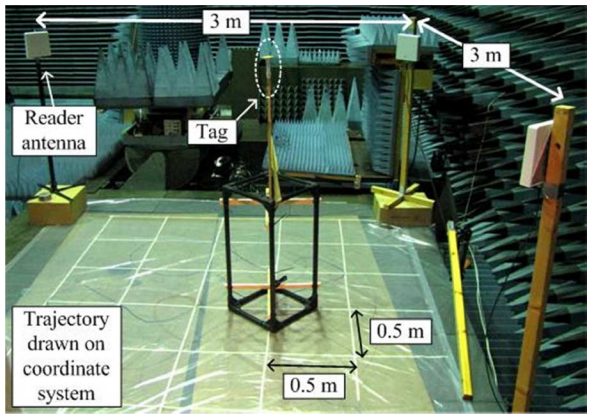


Fig. 3. Photograph of the measurement setup in an anechoic chamber.

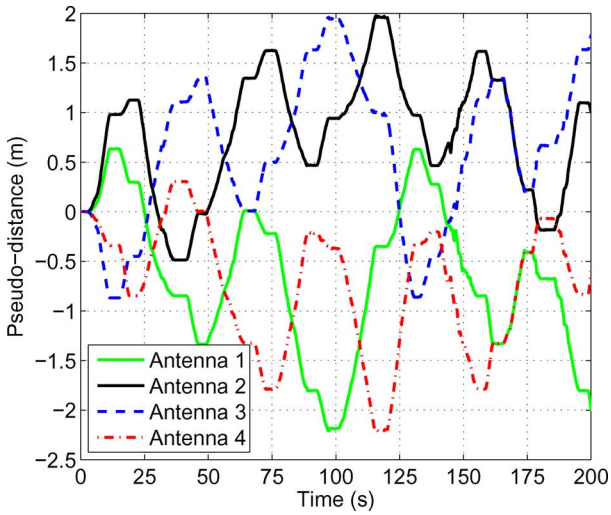


Fig. 4. Pseudo-distances (with unknown constant bias) of the tag from different antennas during one measurement.

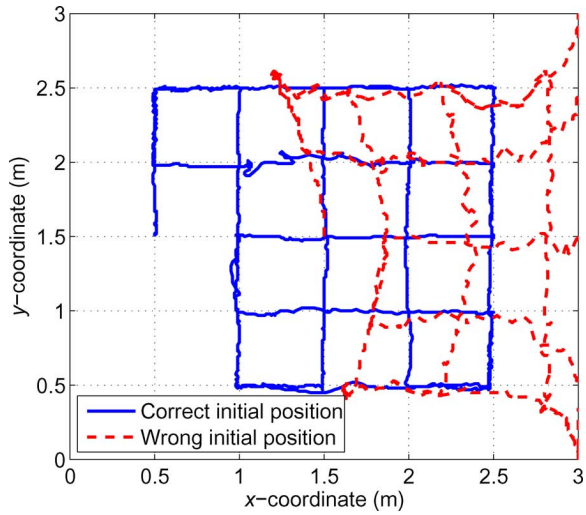


Fig. 5. Trajectory of the tag obtained trilateration with correct (solid blue) and wrong (dashed red) initial position.

In this experiment the tag was moved along the coordinate lines shown in Fig. 5. The solid blue line in Fig. 5 shows the trajectory obtained with a simple point-wise least squares trilateration with the correct initial position. The dashed red line

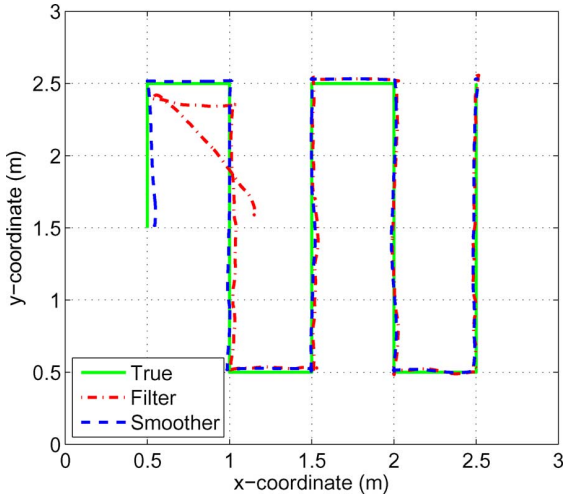


Fig. 6. Experiment 1: trajectories obtained with the EKF (dot dashed red) and RTS smoother (dashed blue) after single iteration.

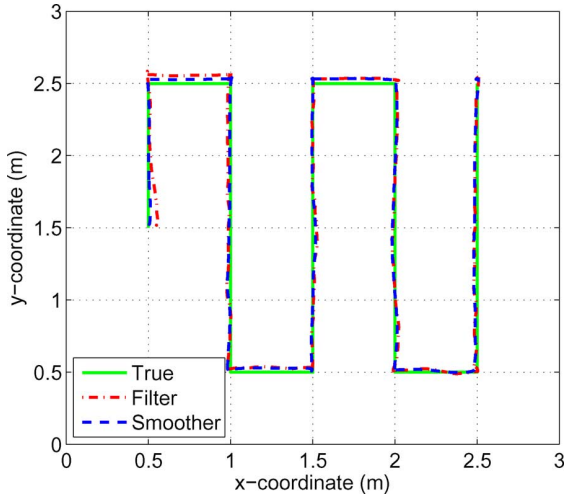


Fig. 7. Experiment 1: trajectories obtained with the EKF (dot dashed red) and RTS smoother (dashed blue) after the second iteration.

shows the same trajectory when the initial position of the tag is unknown and assumed to be in the middle of the measurement area. As can be seen in the figure, the bias in the pseudo-measurement causes a significant nonlinear distortion to the estimated trajectory even though the initial position is only 1 meter off.

### C. Dynamic Tracking Using EKF and Smoother

Fig. 6 shows the estimates produced by EKF and RTS when the initial position is estimated with the RSSI-based method assuming a priori standard deviation of 3 meters. As can be seen in the figure, the EKF estimate starts approximately at a 60 cm distance from the true position. As the tag moves, the estimate converges towards the correct trajectory and ends very close to the true position. The RTS smoother produces a better estimate of the early part of the trajectory. The root mean squared errors (RMSE) of the EKF and RTS position estimates and the intended trajectory are 3.2 cm and 1.5 cm, respectively. However, we estimate that the RMSE between the intended trajectory and the true trajectory is in the order of 1 – 2 cm due to the inaccurate manual movement of the tag.

As discussed in Section II-E, the estimates of EKF and RTS can be improved by setting the initial mean position of filters and smoothers to the estimate produced by RTS on the first round and re-running the algorithms. Fig. 7 shows the results after this iteration. As can be seen in the figure, the EKF estimate is still slightly biased in the beginning due to the remaining inaccuracy of the initial position, but it quickly converges to the right trajectory. The RMSEs of EKF and RTS were roughly 2.2 cm and 1.5 cm after this second iteration and further iterations did not significantly decrease the error.

The accuracy provided by the proposed method is compared to that of the RSSI-based positioning method of Section II-D. The trajectories obtained with the smoother and the RSSI-based method are shown in Fig. 8. The RMSE of the smoother is 1.5 cm and that of the RSSI-method is 35 cm.

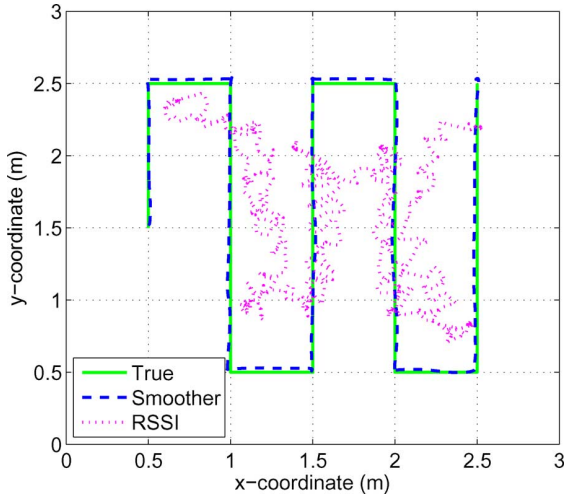


Fig. 8. Experiment 1: trajectories obtained with the RTS smoother (after the third iteration) and the RSSI-based method.

### D. Obtained Trajectories

We recorded different sets of measurements and estimated the position trajectories using the EKF and RTS smoother. In the following Figs. 9–11, we show selected results. In the first of these experiments, the actual trajectory coincided with the coordinate lines and thus we were able to reconstruct the true trajectory in full for visualization and estimation of RMSEs. In the other two experiments, the routes are not aligned with the coordinate lines, but instead, they pass through reference points. The reference points represented with circular markers in the figures.

## IV. Conclusion

In this paper we have presented an UHF RFID tracking system, which is based on measuring phases of backscattered signals at a single carrier frequency from multiple spatially distributed antennas. The phase ambiguity arising from the usage of single frequency is resolved using a state space model for position, velocity and distance offsets, and the states in the model are estimated with EKF and RTSl smoother algorithms.

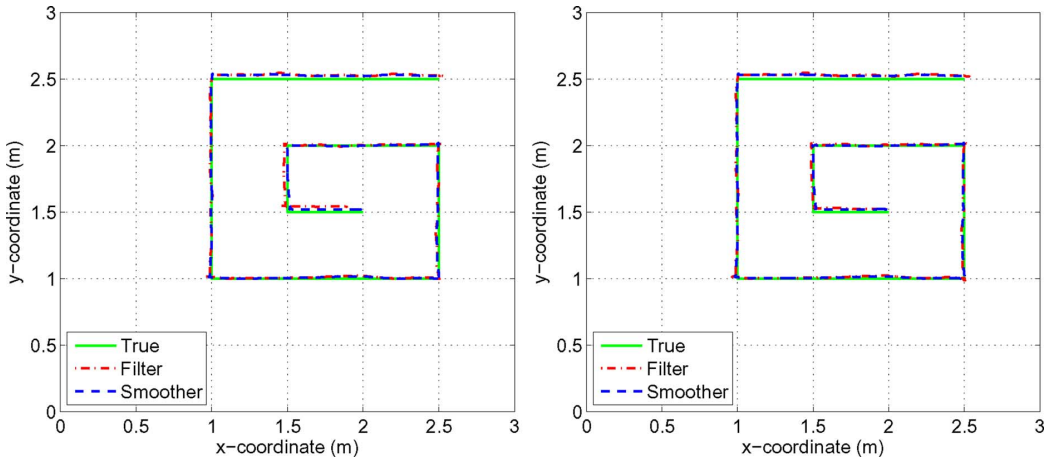


Fig. 9. Experiment 2: Trajectories obtained with the EKF and RTS smoother on the first iteration (left) and on the second iteration (right). The RMSE values were 1.9 cm/1.3 cm for EKF/RTS after the first iteration, respectively, and 1.6 cm/1.3 cm after the second iteration.

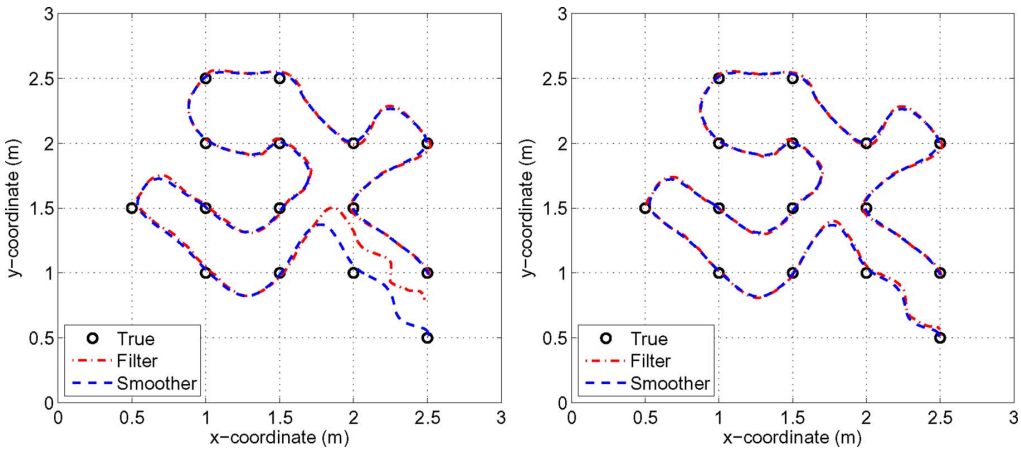


Fig. 10. Experiment 3: Trajectories obtained with the EKF and RTS smoother on the first iteration (left) and on the second iteration (right). The RMSE values were 5.2 cm/1.7 cm for EKF/RTS after the first iteration, respectively, and 1.7 cm/1.3 cm after the second iteration.

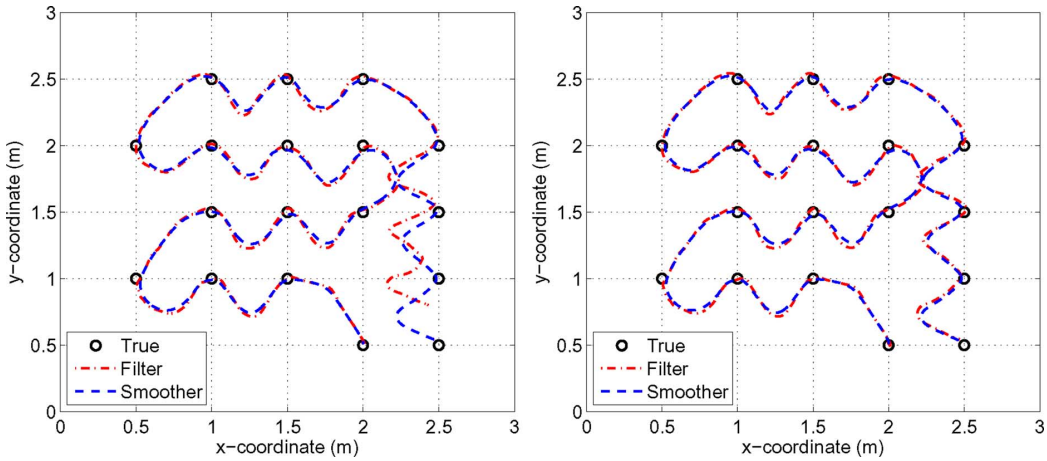


Fig. 11. Experiment 4: Trajectories obtained with the EKF and RTS smoother on the first iteration (left) and on the second iteration (right). The RMSE values were 4.2 cm/2.0 cm for EKF/RTS after the first iteration, respectively, and 1.8 cm/2.0 cm after the second iteration.

The performance of the method was experimentally verified at a carrier frequency of 890 MHz and the results indicate an RMS accuracy of 1–2 centimeters on a 3 m by 3 m square shaped measurement area with 4 antennas in the corners. The deviations are assumed to partly derive from the inaccuracies in the manual movement of the tag.

## REFERENCES


[1] R. Want, A. Hopper, V. Falcao, and J. Gibbons, "The active badge location system," *ACM Trans. Inf. Syst.*, pp. 91–102, Jan. 1992.

[2] A. Harter, A. Hopper, P. Steggles, A. Ward, and P. Webster, "The anatomy of a context-Aware Application," *Wireless Netw.*, vol. 8, no. 2-3, pp. 187–197, Mar. 2002.

[3] V. Viikari, J. Chisum, and H. Seppä, "Wireless passive photo detector for insect tracking," *Microw. Opt. Technol. Lett.*, vol. 52, no. 10, pp. 2312–2315, Oct. 2010.

[4] J. Zhao and Y. Wang, "Autonomous ultrasonic indoor tracking system," in *Proc. Int. Symp. Parallel and Distributed Processing with Applications*, Dec. 10 – 12, 2008, pp. 532–539.

[5] E. Aitenbichler, "A focus on location context," in *Handbook of Research on Ubiquitous Computing Technology for Real Time Enterprises*, M. Muhlhauser and I. Gurevych, Eds. Hershey, PA: IGI Global, 2008, pp. 257–281.

[6] H. Liu, H. Darabi, P. Banerjee, and J. Liu, "Survey of wireless indoor positioning techniques and systems," *IEEE Trans. Syst., Man, Cybern. C: Appl. Rev.*, vol. 37, no. 6, pp. 1067–1080, Nov. 2007.

[7] J. Hightower and G. Borriello, "Location systems for ubiquitous computing," *IEEE Computer*, vol. 34, no. 8, pp. 57–66, Aug. 2001.

[8] J. Hightower, R. Want, and G. Borriello, SpotON: An Indoor 3D Location Sensing Technology based on RF Signal Strength Univ. Washington, Seattle, 2000, Technical report UW CSE 2000-02-02.

[9] L. M. Ni, Y. Liu, Y. C. Lau, and A. P. Patil, "LANDMARC: Indoor location sensing using active RFID," *Wireless Netw.*, vol. 10, no. 6, pp. 701–710, Nov. 2004.

[10] M. Liukku, "UHF-RFID Identification and Positioning of Butterflies," M.Sc. thesis, Helsinki University of Technology, Department of Engineering Physics and Mathematics, Espoo, Finland, 2008.

[11] C. Wang, H. Wu, and N.-F. Tzeng, "RFID-based 3-D positioning schemes," in *Proc. IEEE Int. Conf. Computer Communications*, May 6 – 12, 2007, pp. 1235–1243.

[12] V. Viikari, P. Pursula, and K. Jaakkola, "Ranging of UHF RFID tag using stepped frequency read-out," *IEEE Sensors J.*, vol. 10, no. 9, pp. 1535–1539, Sep. 2010.

[13] ETSI Standard ETSI EN 302 208-1 V1.3.1 2009.

[14] P. V. Nikitin, R. Martinez, S. Ramamurthy, H. Leland, G. Spiess, and K. V. S. Rao, "Phase based spatial identification of UHF RFID tags," in *Proc. 2010 IEEE Int. Conf. RFID*, 2010, pp. 102–109.

[15] Y. Bar-Shalom, X.-R. Li, and T. Kirubarajan*, Estimation with Applications to Tracking and Navigation*. New York: Wiley Interscience, 2001.

[16] J. L. Crassidis and J. L. Junkins*, Optimal Estimation of Dynamic Systems*. London, U.K.: Chapman & Hall/CRC, 2004.

[17] D. R. Reynolds and J. R. Riley, "Remote-sensing, telemetric and computer-based technologies for investigating insect movement: A survey of existing and potential techniques," *Comput. Electron. Agriculture*, vol. 35, pp. 271–307, 2002.

[18] D. E. N. Davies and R. J. Klensch, "Two-frequency secondary radar incorporating passive transponders," *Inst. Elect. Engr. Electron. Lett.*, vol. 9, no. 25, pp. 592–593, Dec. 1973.

[19] E. T. Cant, A. D. Smith, D. R. Reynold, and J. L. Osborne, "Tracing butterfly flight paths across the landscape with harmonic radar," *Proc. Roy. Soc.y B: Biological Sciences*, vol. 272, no. 1565, pp. 785–790, Apr. 2005.

[20] J. R. Riley and A. D. Smith, "Design considerations for an harmonic radar to investigate the flight of insects at low altitude," in *Computers and Electronics in Agriculture*. Amsterdam, The Netherlands: Elsevier, 2002, vol. 35, pp. 151–169.

[21] B. G. Colpitts and G. Boiteau, "Harmonic radar transceiver design: Miniature tags for insect tracking," *IEEE Trans. Antennas Propag.*, vol. 52, no. 11, pp. 2825–2832, Nov. 2004.

[22] [Online]. Available: www.recco.com

[23] V. Viikari and H. Seppä, "RFID MEMS sensor concept based on intermodulation distortion," *IEEE Sensors J.*, vol. 9, no. 12, pp. 1918–1923, Dec. 2009.

[24] V. Viikari, H. Seppä, T. Mattila, and A. Alastalo, "Wireless ferroelectric resonating sensor," *IEEE Trans. Ultrason., Ferroelect. Freq. Contr.*, 2009, to be published.

[25] V. Viikari, H. Seppä, and D.-W. Kim, "Intermodulation read-out principle for passive wireless sensors," *IEEE Trans. Microw. Theory Tech.*, 2010, to be published.

[26] S. J. Julier and J. K. Uhlmann, "Unscented filtering and nonlinear estimation," *Proce. IEEE*, vol. 92, no. 3, pp. 401–422, Mar. 2004.

[27] S. Särkkä, "On unscented Kalman filtering for state estimation of continuous time nonlinear systems," *IEEE Trans. Autom. Contr.*, vol. 52, no. 9, pp. 1631–1641, Sep. 2007.

[28] K. Ito and K. Xiong, "Gaussian filters for nonlinear filtering problems," *IEEE Trans. Autom. Contr.*, vol. 45, no. 5, pp. 910–927, May 2000.

[29] Y. Wu, D. Hu, M. Wu, and X. Hu, "A numerical-integration perspective on Gaussian filters," *IEEE Trans. Sig. Process.*, vol. 54, no. 8, pp. 2910–2921, Aug. 2006.

[30] I. Arasaratnam and S. Haykin, "Cubature Kalman filters," *IEEE Trans. Autom. Contr.*, vol. 54, no. 6, pp. 1254–1269, Jun. 2009.

[31] S. Särkkä, "Unscented Rauch-Tung-Striebel smoother," *IEEE Trans. Autom. Contr.*, vol. 53, no. 3, pp. 845–849, Mar. 2008.

[32] S. Särkkä and J. Hartikainen, "On Gaussian optimal smoothing of nonlinear state space models," *IEEE Trans. Autom. Contr.*, vol. 55, no. 8, pp. 1938–1941, Aug. 2010.


**Simo Särkkä** (S'04–M'06) was born in Tampere, Finland, 1976. He received the Master of Science (Tech.) degree (with distinction) in physics/mathematics and Doctor of Science (Tech.) degree (with distinction) in electrical engineering from Helsinki University of Technology, Espoo, Finland, in 2000 and 2006, respectively.

He is currently a Senior Researcher with the Department of Biomedical Engineering and Computational Science of Aalto University, Espoo, Finland. His research interests are in estimation of stochastic systems, Bayesian methods in signal processing and applications in brain imaging, positioning systems, and audio signal processing.

**Ville V. Viikari** (S'06–A'09–M'09–SM'10) was born in Espoo, Finland, in 1979. He received the Master of Science (Tech.), Licentiate of Science (Tech.) (with distinction), and Doctor of Science (Tech.) (with distinction) degrees in electrical engineering from the Helsinki University of Technology (TKK), Espoo, in 2004, 2006, and 2007, respectively.

From 2001 to 2007, he was with the Radio Laboratory, TKK, where he studied antenna measurement techniques at submillimeter wavelengths and antenna pattern correction techniques. He is currently a Senior Research Scientist with the VTT Technical Research Centre in Espoo, and a Docent (~Adjunct Professor) with the Aalto University, Espoo, Finland. His current research interests are RFID systems and wireless sensors.

Dr. Viikari is the recipient of the IEEE Sensors Council 2010 Early Career Gold Award. He has also received the Young Scientist Award at URSI XXXI Finnish Convention on Radio Science, Espoo, October 28, 2008, and the best student paper award in the annual symposium of the Antenna Measurement Techniques Association, Newport , RI), October 30 – November 4, 2005.

**Miika Huusko** was with the VTT Technical Research Centre of Finland during the research.

**Kaarle Jaakkola** was born in Helsinki, Finland, in 1976. He received the Master of Science (Tech.) degree in electrical engineering from the Helsinki University of Technology (TKK), Espoo, Finland, in 2003.

Since 2000 he has been working with the VTT Technical Research Centre of Finland, currently as a Research Scientist. His current research interests and expertise include RFID systems, wireless and applied sensors, antennas, electromagnetic modelling and RF electronics. He has developed RF parts for RFID systems and designed antennas for both scientific use and commercial products.